NASA/CR—2007-214924

AIAA–2007–3640

Noise Generation in Hot Jets

Abbas Khavaran
ASRC Aerospace Corporation, Cleveland, Ohio

Donald C. Kenzakowski
Combustion Research & Flow Technology, Inc., Pipersville, Pennsylvania

July 2007

NASA STI Program . . . in Profile

Since its founding, NASA has been dedicated to the advancement of aeronautics and space science. The NASA Scientific and Technical Information (STI) program plays a key part in helping NASA maintain this important role.

The NASA STI Program operates under the auspices of the Agency Chief Information Officer. It collects, organizes, provides for archiving, and disseminates NASA's STI. The NASA STI program provides access to the NASA Aeronautics and Space Database and its public interface, the NASA Technical Reports Server, thus providing one of the largest collections of aeronautical and space science STI in the world. Results are published in both non-NASA channels and by NASA in the NASA STI Report Series, which includes the following report types:

- TECHNICAL PUBLICATION. Reports of completed research or a major significant phase of research that present the results of NASA programs and include extensive data or theoretical analysis. Includes compilations of significant scientific and technical data and information deemed to be of continuing reference value. NASA counterpart of peer-reviewed formal professional papers but has less stringent limitations on manuscript length and extent of graphic presentations.

- TECHNICAL MEMORANDUM. Scientific and technical findings that are preliminary or of specialized interest, e.g., quick release reports, working papers, and bibliographies that contain minimal annotation. Does not contain extensive analysis.

- CONTRACTOR REPORT. Scientific and technical findings by NASA-sponsored contractors and grantees.

- CONFERENCE PUBLICATION. Collected papers from scientific and technical conferences, symposia, seminars, or other meetings sponsored or cosponsored by NASA.

- SPECIAL PUBLICATION. Scientific, technical, or historical information from NASA programs, projects, and missions, often concerned with subjects having substantial public interest.

- TECHNICAL TRANSLATION. English-language translations of foreign scientific and technical material pertinent to NASA's mission.

Specialized services also include creating custom thesauri, building customized databases, organizing and publishing research results.

For more information about the NASA STI program, see the following:

- Access the NASA STI program home page at *http://www.sti.nasa.gov*

- E-mail your question via the Internet to *help@sti.nasa.gov*

- Fax your question to the NASA STI Help Desk at 301–621–0134

- Telephone the NASA STI Help Desk at 301–621–0390

- Write to:
  NASA Center for AeroSpace Information (CASI)
  7115 Standard Drive
  Hanover, MD 21076–1320
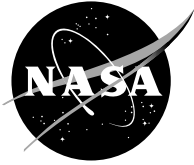
Noise Generation in Hot Jets

Abbas Khavaran
ASRC Aerospace Corporation, Cleveland, Ohio

Donald C. Kenzakowski
Combustion Research & Flow Technology, Inc., Pipersville, Pennsylvania

National Aeronautics and
Space Administration

Glenn Research Center
Cleveland, Ohio 44135

July 2007

Acknowledgments

This report contains preliminary findings,
subject to revision as analysis proceeds.

Level of Review: This material has been technically reviewed by expert reviewer(s).

Noise Generation in Hot Jets

Abbas Khavaran
ASRC Aerospace Corporation
Cleveland, Ohio 44135

Donald C. Kenzakowski
Combustion Research & Flow Technology, Inc. (CRAFT Tech)
Pipersville, Pennsylvania 18947

A prediction method based on the generalized acoustic analogy is presented, and used to evaluate aerodynamic noise radiated from high speed hot jets. The set of Euler equations are split into their respective non-radiating and residual components. Under certain conditions, the residual equations are rearranged to form a wave equation. This equation consists of a third-order wave operator, plus a number of non-linear terms that are identified with the equivalent sources of sound and their statistical characteristics are modeled. A specialized RANS solver provides the base flow as well as turbulence quantities and temperature fluctuations that determine the source strength. The main objective here is to evaluate the relative contribution from various source elements to the far-field spectra and to show the significance of temperature fluctuations as a source of aerodynamic noise in hot jets.

I. Introduction

THERE is ever-increasing demand on the aircraft manufacturers to achieve meaningful levels of noise reduction in order to meet the stringent regulations that are being set for noise emission. To address the noise concerns near airports, NASA introduced a stretched "pillar" goal in 1997, with a stated goal of reducing the perceived noise levels of the future aircraft by 20 EPNdB by 2022 relative to 1994 technology. Jet noise is of particular interest because of its dominant contribution to the community noise at the high thrust conditions during takeoff. As part of an ongoing research effort at the NASA Glenn Research Center, a statistical-based jet noise prediction methodology (JeNo code) is being developed to provide the state-of-the-art in the source modeling and propagation. Since jet mixing-noise is broadband, with frequencies that cover significant levels of noise within three octave band, a successful predictive capability needs to incorporate sufficient physics to produce a reasonably accurate spectrum over a broad range of conditions. The goal is to achieve practical levels of accuracy in noise prediction from this more generalized modeling methodology to help designers with concept evaluation and down selection within a reasonable time frame.

Predicting and suppressing noise from heated jets is of particular interest in aeroacoustics since this is the condition under which real engines operate. In an earlier study [Ref. 1], an acoustic analogy methodology was presented based on the premise that an identified fluctuating velocity/enthalpy source term was a major heat-related source contribution in hot jets. The present paper aims to further examine individual source terms in an inhomogeneous variable density Pridmore-Brown wave equation for their relative contribution to the far-field jet noise spectra. Lighthill [Ref. 2] defined the equivalent sources of aerodynamic noise as the double divergence of the stress tensor $T_{ij} = \rho v_i v_j + (p - c_\infty^2 \rho)\delta_{ij} - \tau_{ij}$, where ρ denotes the density, $\vec{v} = (v_1, v_2, v_3)$ is the fluid velocity, p is the pressure, c_∞ is the ambient speed of sound, and τ_{ij} denotes the viscous stress tensor. This definition has been a subject of wide-spread scrutiny and interpretations and has led to scaling laws that relate the far-field sound to flow parameters such as velocity and temperature in a variety of forms. The viscous stresses are usually considered to be unimportant in noise generation and the momentum flux term $\partial^2 \rho v_i v_j / \partial^2 x_i x_j$ is regarded as the primary source of sound in isothermal jets. Heat addition has a multitude of effects on noise that depends on the jet velocity, frequency, and angle. Experimental observations [Refs. 3,4,5] show that at high speeds (i.e., above acoustic Mach numbers of 0.9), heat addition results in noise reduction at all frequencies. At low speeds, nominally

acoustic Mach number of 0.50 and below, it amplifies the low to mid frequency jet noise with minimal effect at the high frequency. In between, e.g. at acoustic Mach number of 0.70, the spectrum shows a cross-over relative to the unheated case that indicates an enhancement of the low-frequency noise and slight weakening of the high-frequency amplitude.

These observations have compelled many researchers in the field to examine the pressure/density difference $(p - c_\infty^2 \rho)$ that appears in Lighthill's stress tensor [Ref. 2], as a potential contributing source and formulate scaling laws that resemble the usual U^8 law suggested based on the first source term. Some recent examination of jet noise data [6, 7] conclude a more general power law $A U^n$, where the amplitude A and exponent n are parameters that depend on angle and jet stagnation temperature. Morfey *et al*. [8] revised Lush and Fisher's [9] version of entropy source term and offered a new two-scaling hypothesis, in favor of U^6 and U^4 power laws, and with some dependence on the mean temperature gradient. Additionally, they attempted to account for the mean flow effects by using a simplified form of the Geometric Acoustic approximation. Lilley [10] proposed a second order wave equation for the pressure fluctuations, similar to Lighthill's, but replaced $(p - c_\infty^2 \rho)$ with a different expression that explicitly displays its isentropic and non-isentropic components. His new contribution to the total acoustic power consisted of a Dipole term with U^6 dependency, which also multiplied the variance of the total enthalpy. He provided some estimate of the relevance of the new source term without actually calculating the required enthalpy fluctuations

The acoustic equations described in the following section are derived from equations of motion after each flow variable is decomposed into its base flow and radiating components. The Euler equations, rewritten within the framework of Goldstein's generalized acoustic analogy [Ref. 11], are expressed as two set of equations that govern a non-radiating background flow plus its residuals. The residuals components are simply the difference between the original dependent variables and their base-flow equivalents. These are later rearranged to form alternate analogies, and equivalent sources of sound are identified with the non-linear terms in each analogy. Of key significance in the current study, all analogies include, among other factors, a fluctuating velocity/enthalpy term as a heat-related source component.

The non-radiating base flow alluded to above is taken to be the jet mean flow as calculated from a specialized RANS solver that predicts the variance in total temperature (or enthalpy) in addition to the standard turbulence-related parameters. The approach, which is discussed in [Ref. 12], makes use of a baseline k-ε turbulence model demonstrated in past work to predict correct mean flow velocity mixing and turbulent kinetic energy for heated and unheated subsonic round jets. A generalized two-equation scalar variance model is available [Ref. 12] within this turbulence model framework, which utilizes an independent dissipation rate equation as well as the locally available turbulent velocity and time-scale information. Determination of the scalar variance variable is principally achieved by selecting the appropriate mean flow quantity gradient for its production source term (Appendix-A). In the past, this model has been used to predict the local variations in the turbulent Prandtl number and to study its impact on jet thermal mixing using an energy variance approach that tracked the variance in static temperature. The current study traces the variance of the total enthalpy instead as the parameter of interest for subsequent jet noise predictions. The stagnation temperature fluctuations are then deduced from this quantity. The difference between utilizing static versus stagnation fluctuation values for noise prediction becomes increasingly obvious with jet speed. Specifically, a noticeable static temperature variance appears within the jet shear layer for unheated conditions at high exhaust speeds, compared to a practically insignificant total temperature variance. From the standpoint of turbulence model generality, it is interesting to note that, at least for the jet cases studied, the use of total enthalpy variance does not significantly alter predictions for variable turbulent Prandtl number. The local turbulent thermal diffusivity is partially determined from the thermal time-scale; the predicted values for the variance dissipation rate are also affected proportionately by the scalar variance production term selection.

The remainder of this paper is organized as follows. The governing acoustic equations and the sources of jet noise in the specialized case of a locally parallel mean flow are presented in section 2. A summary of the baseline scalar variance model governing the transport of total temperature variance and its dissipation rate is provided in Appendix A. Details regarding the model development can be found in [Refs. 12 and 13]. Section 3 illustrates the sensitivity of stagnation temperature variance to heated and exit velocity conditions for a number of round jets. A comprehensive study of the relative strength of various source components and their far-field noise at 90° is presented in section 4. The comparisons cover a host of subsonic jets in an attempt to identify the most significant sound sources for a wide range of conditions. Source statistics and modeling features appear in

Appendices B and C. The current prediction methodology is calibrated around two source components only, and sample results are presented in section 4.

II. Acoustic Analogies

The details provided here are for completeness and for drawing attention to the underlying assumptions and noise sources in each analogy. Spectral predictions use a third-order inhomogeneous wave equation. This equation assumes a locally parallel mean flow, and consists of a linear wave operator that accounts for the refraction of sound due to flow in-homogeneities, plus a host of source terms that are all non-linear in fluctuating variables (i.e., velocity and total enthalpy fluctuations).

We neglect the non-isentropic effects considering that fluid viscosity and heat conduction play a relatively insignificant role in noise generation. The conservative form of Euler equations

$$\frac{\partial \rho}{\partial t} + \frac{\partial}{\partial x_j} \rho v_j = 0 , \tag{1a}$$

$$\frac{\partial}{\partial t} \rho v_i + \frac{\partial}{\partial x_j} \rho v_i v_j + \frac{\partial p}{\partial x_i} = 0 , \tag{1b}$$

$$\frac{\partial}{\partial t} (\rho h_t - p) + \frac{\partial}{\partial x_j} \rho v_j h_t = 0 , \tag{1c}$$

are linearized about a suitable background flow, and expressed as two set of equations that govern a non-radiating base flow and its residuals. The residual equations are the difference between the original Euler equations and the base-flow relations, and govern the small fluctuations that relate to the generation of sound.

Assuming that the equation of state is governed by the ideal gas law

$$p = \rho \Re T , \tag{2}$$

each flow variable is divided into its mean and fluctuating components as

$$p = \overline{p} + p', \quad \rho = \overline{\rho} + \rho', \quad v_i = \tilde{v}_i + v_i', \quad h = \tilde{h} + h' . \tag{3}$$

The over-bar is a time-averaged value, and tilde denotes a Favre-averaged (i.e., mass-averaged) quantity for all variables including the stagnation enthalpy

$$h_t = h + \frac{1}{2} v^2 , \quad h_t = \tilde{h}_t + h_t', \quad \overline{h_t'} = 0 . \tag{4a}$$

The following expressions are concluded for the Favre-averaged stagnation enthalpy $\tilde{h}_t$ and fluctuations h_t'

$$\tilde{h}_t = \tilde{h} + \frac{1}{2} \tilde{v}^2 + \frac{1}{2} \widetilde{v'^2} , \quad h_t' = h' + \frac{1}{2} v'^2 - \frac{1}{2} \widetilde{v'^2} + \tilde{v}_i v_i' . \tag{4b}$$

The averaged static enthalpy satisfies the averaged ideal gas law

$$\tilde{h} = c_p \tilde{T} , \quad \overline{p} = \Re \overline{\rho} \, \tilde{T} , \tag{4c}$$

and upon subtracting (4c) from Eq. (2), the residual part of the ideal gas law becomes

$$p' = \frac{\Re}{c_p}(\rho h' + \rho' \tilde{h}), \qquad h' = c_p T',$$

(4d)

where c_p and c_v denote the specific gas constants (i.e., $c_p = \gamma c_v$). Equation (4d) shows that density and temperature fluctuations act in concert to generate pressure fluctuations. This is also seen from the equation of state by taking its total differential

$$\frac{dp}{p} = \frac{dT}{T} + \frac{d\rho}{\rho}.$$

(4e)

If the gas were to expand slowly enough to make it possible for the temperature to remain constant, then dT would have to remain as zero, and according to (4e) pressure and density would have to relate as $dp/p = d\rho/\rho$. However, the expansion and contraction of sound waves happen on rapid scale. It is more appropriate to assume that the thermal energy has very little time to flow, and so the expansion occurs adiabatically. Additionally, when the viscous effects are small, sound generation should be regarded as an isentropic process, resulting in pressure/density relationship $dp/p = \gamma(d\rho/\rho)$. Therefore, in view of (4e), changes in pressure and temperature relate as $dp/p = \gamma/(\gamma-1)(dT/T)$.

The analysis shows that density fluctuations may also be replaced with their equivalent in terms of velocity fluctuations from the continuity equation. With the aid of momentum and energy equations, the pressure fluctuations are subsequently expressed in terms of velocity and thermal fluctuations.

The set of Euler's equations are averaged using the above definitions. The averaged equations, herein referred to as the base-flow equations are

$$D_o \bar{\rho} = 0,$$

(5a)

$$D_o (\bar{\rho} \tilde{v}_i) + \frac{\partial \bar{p}}{\partial x_i} = -\frac{\partial}{\partial x_j} \overline{\rho v_i' v_j'},$$

(5b)

$$D_o (\bar{\rho} \tilde{h}_t) - \frac{\partial \bar{p}}{\partial t} = -\frac{\partial}{\partial x_j} \overline{\rho v_j' h_t'}.$$

(5c)

To obtain a self-contained system of equations for the base flow, energy equation (5c) is rearranged as

$$D_o \left(\bar{\rho}(\tilde{h} + \frac{1}{2} \tilde{v}^2) \right) - \frac{\partial \bar{p}}{\partial t} = -\frac{\partial}{\partial x_j} \overline{\rho v_j' h_t'} - \frac{1}{2} D_o (\overline{\rho v_j' v_j'})$$

(5d)

The base flow is solved by modeling the stress terms on the RHS of (5b) and (5d) and using the ideal gas law $(\gamma - 1)\bar{\rho} \tilde{h} = \gamma \bar{p}$. In a RANS-type mean flow we require $\partial \bar{p} / \partial t = 0$. Upon subtracting the above equations from the set of equations (1), the following relations (referred to as the residual equations) are found for the fluctuating variables

$$D_o \rho' + \frac{\partial m_j}{\partial x_j} = 0,$$

(6a)

$$D_o m_i + D_o (\rho' \tilde{v}_i) + \frac{\partial p'}{\partial x_i} + \frac{\partial}{\partial x_j}(m_j \tilde{v}_i) = \frac{\partial e_{ij}}{\partial x_j},$$

(6b)

$$D_o (\rho' \tilde{h}_t + \rho h_t') + \frac{\partial}{\partial x_j}(\rho v_j' h_t) - \frac{\partial p'}{\partial t} = \frac{\partial}{\partial x_j} \overline{\rho v_j' h_t'}.$$

(6c)

We have used the following definitions

$$D_o f \equiv \frac{\partial f}{\partial t} + \frac{\partial}{\partial x_j}(\tilde{v}_j f) \tag{7a}$$

$$m_j \equiv \rho v_j' \tag{7b}$$

$$e_{ij} \equiv -(\rho v_i' v_j' - \overline{\rho v_i' v_j'}) . \tag{7c}$$

The energy equation is now written in a different form that is more closely related to pressure fluctuations p'. Using the ideal gas law (4d), the first term on the LHS of the energy equation (6c) is recognized as

$$(\rho' \tilde{h}_t + \rho h_t') = \frac{\gamma}{\gamma - 1} p' + m_j \tilde{v}_j + \frac{1}{2}(\rho' \tilde{v}^2 - e_{jj}) . \tag{7d}$$

For later derivation of the convective wave equation, it is also more appropriate to express time derivative $\partial p'/\partial t$ in (6c) in terms of the operator D_o

$$\frac{\partial p'}{\partial t} = D_o p' - p' \frac{\partial \tilde{v}_i}{\partial x_i} - \tilde{v}_i \frac{\partial p'}{\partial x_i} . \tag{8}$$

We substitute for $\partial p'/\partial x_i$ from (6b) into (8), and subsequently place $\partial p'/\partial t$ from (8) into (6c) to obtain the following energy equation

$$\frac{1}{\gamma - 1} D_o p' + \frac{\partial}{\partial x_j}(m_j \tilde{h}) + p' \frac{\partial \tilde{v}_j}{\partial x_j} + \tilde{v}_i m_j \frac{\partial \tilde{v}_j}{\partial x_i} = \frac{1}{2} D_o e_{jj} - \tilde{v}_j \frac{\partial e_{ij}}{\partial x_i} - \frac{\partial}{\partial x_j}(\rho v_j' \hbar_t' - \overline{\rho v_j' \hbar_t'}) \tag{9a}$$

where

$$\hbar_t' \equiv h_t' + \frac{1}{2}\widetilde{v'^2} \tag{9b}$$

The energy equation (9a) may also be written in a slightly different form using a new variable h_o' that is related to the actual fluctuation in stagnation enthalpy h_t' as

$$h_o' \equiv h' + \frac{1}{2}v'^2 = h_t' + \frac{1}{2}\widetilde{v'^2} - \tilde{v}_i v_i' \tag{9c}$$

Substituting (9c) into (9a), the energy equations becomes

$$\frac{1}{\gamma - 1} D_o p' + \frac{\partial}{\partial x_j}(m_j \tilde{h}) + p' \frac{\partial \tilde{v}_j}{\partial x_j} + \tilde{v}_i m_j \frac{\partial \tilde{v}_j}{\partial x_i} = \frac{1}{2} D_o e_{jj} + e_{ij} \frac{\partial \tilde{v}_j}{\partial x_i} - \frac{\partial}{\partial x_j}(\rho v_j' h_o' - \overline{\rho v_j' h_o'}) \tag{9d}$$

Alternate definitions for the dependent variables are possible at the cost of re-defining the source. For example, the first term on the RHS of the energy equation (9d) may be combined with the leading term on the LHS to define a new pressure variable [Ref. 11] as $p_e' = p' - (\gamma - 1)e_{kk}/2$

$$\frac{1}{\gamma-1}D_o p'_e + \frac{\partial}{\partial x_j}(m_j \tilde{h}) + p'_e \frac{\partial \tilde{v}_j}{\partial x_j} + \tilde{v}_i m_j \frac{\partial \tilde{v}_j}{\partial x_i} = (e_{ij} - \frac{\gamma-1}{2}e_{kk}\delta_{ij})\frac{\partial \tilde{v}_j}{\partial x_i} - \frac{\partial}{\partial x_j}(\overline{\rho v'_j h'_o} - \overline{\rho v'_j h'_o}). \quad (9e)$$

With respect to the generalized pressure p'_e, the momentum equation (6b) becomes

$$D_o m_i + D_o(\rho' \tilde{v}_i) + \frac{\partial p'_e}{\partial x_i} + \frac{\partial}{\partial x_j}(m_j \tilde{v}_i) = \frac{\partial}{\partial x_j}(e_{ij} - \frac{\gamma-1}{2}e_{kk}\delta_{ij}). \quad (9f)$$

A. Special Cases of the Acoustic Equation

Consider the case when the mean flow is parallel and a function of the span-wise coordinates only

$$\tilde{v}_j = \delta_{j1}U(x_2, x_3), \quad \overline{\rho} = \overline{\rho}(x_2, x_3), \quad \overline{p} = \text{constant}, \quad (10)$$

subsequently

$$D_o = D = \frac{\partial}{\partial t} + U \frac{\partial}{\partial x_1}. \quad (11a)$$

Using the ideal gas law, we have

$$(\gamma-1)\overline{\rho}\,\tilde{h} = \gamma \overline{p} = \overline{\rho}\widetilde{c^2}. \quad (11b)$$

And the base flow momentum equation (5b) shows that

$$\frac{\partial}{\partial x_j}\overline{\rho v'_i v'_j} = 0. \quad (12a)$$

Then according to Eq. (4b)

$$\tilde{h}_t = \tilde{h}(x_2, x_3) + \frac{1}{2}U^2(x_2, x_3) + \frac{1}{2}\widetilde{v'^2}. \quad (12b)$$

And the base flow energy equation shows that

$$\frac{1}{2}U\frac{\partial}{\partial x_1}(\overline{\rho}\widetilde{v'^2}) + \frac{\partial}{\partial x_j}\overline{\rho v'_j h'_t} = 0. \quad (12c)$$

Using the above results into the residual momentum and energy equations we conclude

$$\frac{\partial p'}{\partial x_i} + Dm_i + \delta_{i1}m_j \frac{\partial U}{\partial x_j} = \frac{\partial e_{ij}}{\partial x_j}, \quad (13)$$

$$Dp' + \frac{\partial}{\partial x_j}(\widetilde{c^2}m_j) = q, \quad (14)$$

where

$$q \equiv -(\gamma-1)\left(\frac{1}{2}D(\overline{\rho v'^2}) + \frac{\partial}{\partial x_j}(\overline{\rho v'_j h'_t}) - U\frac{\partial}{\partial x_j}(\overline{\rho v'_1 v'_j})\right). \quad (15a)$$

Source expression q may also be expressed in terms of h'_o as defined in (9c)

$$q \equiv -(\gamma - 1)\left(\frac{1}{2} D(\rho v'^2) + \frac{\partial}{\partial x_j}(\rho v'_j h'_o) + (\rho v'_i v'_j)\frac{\partial U}{\partial x_j}\right) \tag{15b}$$

Residual parts of the continuity (6a), momentum (13), and energy equation (14) are now rearranged to construct wave equations for either pressure or density.

A form of Phillips' equation is derived after eliminating factor m_j between momentum and energy equations by taking the convective derivative of the latter and subtracting that from the gradient of the former

$$D^2 p' - \frac{\partial}{\partial x_j}(\widetilde{c^2}\frac{\partial p'}{\partial x_j}) = -\frac{\partial}{\partial x_i}(\widetilde{c^2}\frac{\partial e_{ij}}{\partial x_j}) + 2\widetilde{c^2}\frac{\partial U}{\partial x_i}\frac{\partial m_i}{\partial x_1} + Dq. \tag{16}$$

Lilley's second-order wave equation for acoustic pressure in a *stationary* mean flow [Refs. 10, 14] is deduced from Eq. (16) if we let $U = 0$, $\widetilde{c^2} = c_\infty^2$, and $\overline{p} = p_\infty$ (note that $h'_t = h'_o$ in a stationary mean flow)

$$\frac{\partial^2 p'}{c_\infty^2 \partial t^2} - \frac{\partial^2 p'}{\partial x_j \partial x_j} = \frac{\partial^2 (\rho v'_i v'_j)}{\partial x_i \partial x_j} - \frac{\gamma - 1}{2c_\infty^2}\frac{\partial^2 (\rho v'^2)}{\partial t^2} - \frac{\partial^2}{\partial x_j \partial t}(\frac{\rho v'_j h'_o}{h_\infty}), \tag{17}$$

where $(\gamma - 1)h_\infty = c_\infty^2$. Since the sound speed was set equal to that measured at the far-field observer point, the

mean density needs to be equal to the ambient density $\rho = \rho_\infty = \gamma p_\infty / c_\infty^2$ as well. Therefore the actual jet density does not have a place in the source.

Similarly, Lighthill's equation for density fluctuations in a quiescent medium ($U = 0$, $\widetilde{c^2} = c_\infty^2$, and $\overline{p} = p_\infty$) is written after eliminating $\partial^2 m_j / \partial t \partial x_j$ between continuity and momentum Eqs (6a) and (13)

$$\frac{\partial^2 \rho'}{\partial t^2} - c_\infty^2 \frac{\partial^2 \rho'}{\partial x_j \partial x_j} = \frac{\partial^2}{\partial x_i \partial x_j}\left[\rho v'_i v'_j + (p' - c_\infty^2 \rho')\delta_{ij}\right]. \tag{18}$$

Again ρ should be set equal to the ambient density ρ_∞. Notice that unlike the conventional acoustic analogy, the base-flow equation is already subtracted from Eq. (18), and the sources on the right hand side consist of fluctuating terms only. The pressure/density difference that appears as a source in Lighthill's equation is second-order in fluctuating variables, and may be written after eliminating $\partial m_j / \partial x_j$ between continuity and energy equations (6a) and (14). A form of Lighthill's acoustic analogy that accounts for the energy equation would be a third-order wave equation

$$\frac{\partial}{\partial t}\left[\frac{\partial^2 \rho'}{\partial t^2} - c_\infty^2 \frac{\partial^2 \rho'}{\partial x_j \partial x_j}\right] = \rho_\infty \frac{\partial^2}{\partial x_i \partial x_j}\left[\frac{\partial}{\partial t}v'_i v'_j - (\gamma - 1)\left(\frac{1}{2}\frac{\partial}{\partial t}v'^2 + \frac{\partial}{\partial x_k}v'_k h'_o\right)\delta_{ij}\right]. \tag{19}$$

A comparison of equations (17) and (19) clearly shows that pressure fluctuations may be viewed as a preferred parameter in writing the wave equation.

The source components in equation (17) when calculated on a proper surface (i.e., $U \simeq 0$) may be used in conjunction with the Kirchhoff approach or Ffowcs-Wiliams/Hawkings (FWH) surface integral methods to calculate the far-field acoustic pressure. The difference between the above source and the usual acoustic analogy (18) is that Eq. (17) requires time history of the velocity and the stagnation enthalpy on the surface.

Rather than assuming a quiescent acoustic medium, it is more appropriate to include the mean flow effect by moving the linear component from the second source term on the right hand side of Phillips' equation (16) to its operator side. To realize this, form the axial gradient $\partial/\partial x_1$ of the momentum equation (13), multiply that by $\partial U/\partial x_i$, and subtract the result from the convective derivative of Eq. (16) to obtain the third-order convective wave equation

$$D \left[D^2 p' - \frac{\partial}{\partial x_j}(\widetilde{c^2}\frac{\partial p'}{\partial x_j}) \right] + 2\widetilde{c^2}\frac{\partial U}{\partial x_j}\frac{\partial^2 p'}{\partial x_1 \partial x_j} =$$
$$- D\frac{\partial}{\partial x_i}(\widetilde{c^2}\frac{\partial e_{ij}}{\partial x_j}) + 2\widetilde{c^2}\frac{\partial U}{\partial x_j}\frac{\partial^2 e_{ij}}{\partial x_1 \partial x_i} + D^2 q. \tag{20}$$

Stress terms e_{ij} and q were defined in Eqs. (7c) and (15). This result, also referred to as an inhomogeneous Pridmore-Brown equation, is expressed in a more transparent form as

$$Lp' = \Gamma , \tag{21}$$

where source expression Γ was defined as the RHS of Eq. (20) and the operator L is

$$L \equiv D(D^2 - \frac{\partial}{\partial x_j}\widetilde{c^2}\frac{\partial}{\partial x_j}) + 2\widetilde{c^2}\frac{\partial U}{\partial x_j}\frac{\partial^2}{\partial x_1 \partial x_j} . \tag{22}$$

Equation (20) may also be derived directly by rearranging equation (3.5) of [Ref. 11] .

A comparison of equations (20) and (17) shows that the presence of a mean flow not only refracts the sound after it was generated, but it also modifies the sources of sound as evidenced by the RHS of these two equations.

B. Discussion

The acoustic equations described above are all consistent in their description of the aerodynamic noise sources. With the exception of Phillips' equation (16) which still holds a linear term on the right hand side, the subsequent wave equations (17), (19) and (20) are summarized as $Lq = s$, where the linear operator L acts on either pressure or density fluctuations, and the source s consists of components that are, at least, second-order in fluctuating variables. These equations were derived from the residual continuity, momentum and energy equations (6a, 13, 14); and as such their respective sources should be viewed as the difference between the more traditional analogies and their non-radiating base flow. In conventional analogies, source consists of both linear and non-linear components [Refs. 15,16,17]. In the following, additional simplification is provided prior to an assessment of individual source elements.

C. Further Simplification of the Acoustic Equation

The source expression in the convective wave equation (20) is further simplified once we insert the assumption of a locally parallel mean flow into the base-flow equations and conclude that Reynolds stress $\rho v_i' v_j'$ has a Favre-averaged value that is independent of the source location. While this simplifications leaves out the gradients

of $\overline{\rho v_i' v_j'}$ from the source elements in Eq. (20), it is still realized that in a real spreading jet, base-flow momentum and energy equations are both inhomogeneous, which implies that the true sources are the difference between the fluctuating and Favre-averaged Reynolds stresses and enthalpy fluxes. Subsequently we let

$$\frac{\partial e_{ij}}{\partial x_j} = -\frac{\partial}{\partial x_j}(\rho v_i' v_j') . \tag{23}$$

In a RANS-based jet noise prediction, the base flow is usually the averaged mean flow. The two-point statistics between various fluctuating variables are modeled and calculated from their respective variance combined with the time- and length-scales of the local turbulence. Thus the density factor ρ appearing in the numerator of each source component in Eq. (20) is replaced with its mean value $\overline{\rho}$, which practically amounts to neglecting terms that are higher than second-order in fluctuating variables. Dividing equation (20) by constant $\gamma \overline{p}$ one finds

$$L\pi' = \Gamma, \qquad \pi' \equiv \frac{p'}{\gamma \overline{p}} \tag{24}$$

where the *equivalent* sources of aerodynamic sound are

$$
\Gamma \cong D \left(\overbrace{\frac{\partial^2 v_i' v_j'}{\partial x_i \partial x_j}}^{I} - \overbrace{\frac{1}{2} D^2 (\frac{v'^2}{\tilde{h}})}^{II} \right) \qquad \text{self}
$$

$$
-2\frac{\partial U}{\partial x_j} \left(\overbrace{\frac{\partial^2 v_i' v_j'}{\partial x_1 \partial x_i}}^{I} + \overbrace{\frac{1}{2} D^2 (\frac{v_1' v_j'}{\tilde{h}})}^{II} + \overbrace{(\frac{1}{\overline{\rho}} \frac{\partial \overline{\rho}}{\partial x_i}) \frac{\partial}{\partial x_1} (v_i' v_j')}^{III} \right) \qquad \text{shear} \tag{25}
$$

$$
- D \left(\overbrace{D \frac{\partial}{\partial x_j} (v_j' \frac{h_o'}{\tilde{h}})}^{I} - \overbrace{\frac{\partial}{\partial x_j} (\frac{v_i' v_j'}{\overline{\rho}} \frac{\partial \overline{\rho}}{\partial x_i})}^{II} \right) . \qquad \text{enthalpy}
$$

Three pairs of brackets in equation (25) designate three distinct sources. The former terms in each bracket are identified as self, shear, and enthalpy sources respectively. Self and shear source terms are second-order in fluctuating velocity, and are each complemented by a second term involving the mean flow enthalpy which is not zero even when the flow is isothermal, but is shown to be small relative to the former. Source terms that consist of the mean density gradient are negligible in unheated jets, but could potentially become important as jets get hot. The second source component within the enthalpy noise group was originally part of the first source term in equation (20); and is now grouped with the heat-related sources. A detailed comparison of the individual source terms of Eq. (25) is presented in the next section. It turns out that the major difference between the unheated and heated jets is due to the fluctuations in stagnation enthalpy that appears in the third bracket above. This term is first order in velocity fluctuations, and its spectral shape behaves as ω^4 in the low frequency limit, and its high-frequency roll-off could be modeled to behave as ω^{-3}, similar to the self noise.

III. Subsonic Flowfield Simulations

A total of eight subsonic cases within the Tanna matrix [Ref. 18] were considered for simulation of a 2-inch diameter jet using the total enthalpy variance model (Appendix A). The nozzle exhaust conditions as defined by set

points within the Tanna matrix are summarized in Table I. In past work, these cases were studied extensively [Ref. 19] to better understand and predict turbulence quantities in the developing jet region, where most of the jet noise is produced. Comparisons were made with available PIV data collected at the SHJAR facility [Refs. 4,20] at NASA/Glenn Research Center. Sample results that compares energy variance model with the total enthalpy variance model were presented in a previous study [Ref. 1].

Simulations use an axisymmetric 316x171 computational grid, which includes the internal nozzle region well upstream of the exit plane. The computational domain extends 100 jet exit radii in the streamwise direction and 25 jet exit radii radially, sufficiently distant to minimize boundary condition placement impact on the shear layer entrainment path-lines. Nozzle flow boundary conditions were prescribed uniformly as inflow stagnation conditions for pressure and temperature imposed well upstream of the nozzle exit. Solution grid resolution sensitivity and convergence criteria were discussed in [Ref. 1]. The same reference also compares fluctuations in total and static temperatures and shows that the former parameter remains consistently small in unheated jets while the latter could grow to become significant with jet speed. The predicted centerline decay of mean axial velocity and turbulent kinetic energy are plotted in Figure 1 as a function of Witze axial parameter x_w for subsonic jets [Ref. 21]. The length of the potential core collapses at $x_w/r_j \cong 1$ in agreement with the theory – and the peak TKE on the centerline is at $x_w/r_j \cong 1.5$, and shows slight increase with jet temperature.

$$x_W = 0.08\left(\sqrt{\frac{\rho_\infty}{\rho_j}} - 0.16\frac{U_j}{c_\infty}\right)\left(\frac{\rho_\infty}{\rho_j}\right)^{-0.22} x \tag{26}$$

Contour plots in Figures 2 and 3 show the variance in total temperature for the first 15-diameters of the jet as a function of jet speed and temperature. The peak temperature fluctuations increase with both speed and temperature. Similar calculations in unheated jets show that peak levels of 0.20x10-2 and 0.70x10-2 for cases sp03 and sp07 are relatively insignificant within the context of the heated jets.

Table I. Tanna Matrix Set Point Conditions

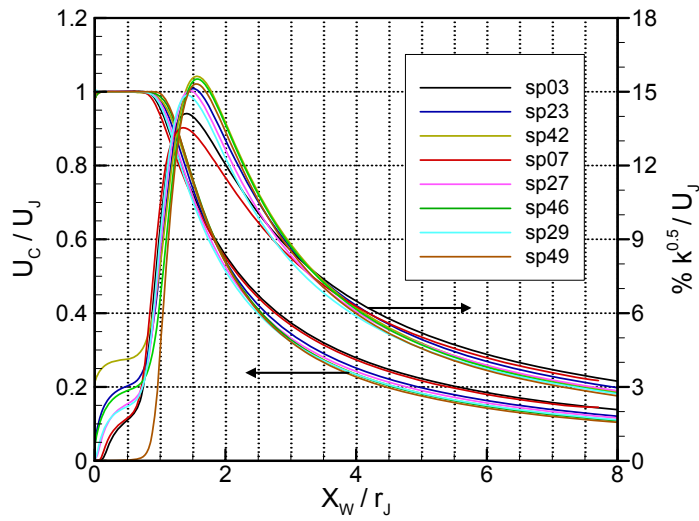| S.P.	NPR	$T_{t,j}/T_\infty$	T_j/T_∞	M_{ac}^*	M_j
03	1.197	1.000	0.950	0.50	0.51
23	1.103	1.810	1.760	0.50	0.37
42	1.066	2.750	2.700	0.50	0.30
07	1.861	1.000	0.840	0.90	0.98
27	1.361	1.922	1.760	0.90	0.68
46	1.225	2.861	2.700	0.90	0.54
29	1.900	2.114	1.760	1.33	1.00
49	1.692	3.138	2.700	1.48	0.90

$$^*M_{ac} = U_j/c_\infty$$

Figure 1. Centerline velocity and turbulent kinetic energy vs. Witze axial parameter in subsonic jets.
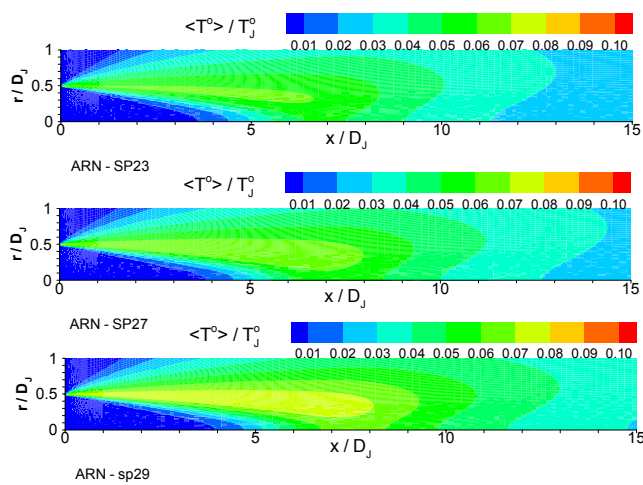

Figure 2. Variance in total temperature normalized with exit total temperature at static temperature ratio of 1.76 and jet acoustic Mach number of: 0.50 (top); 0.90 (middle); and 1.33 (bottom).
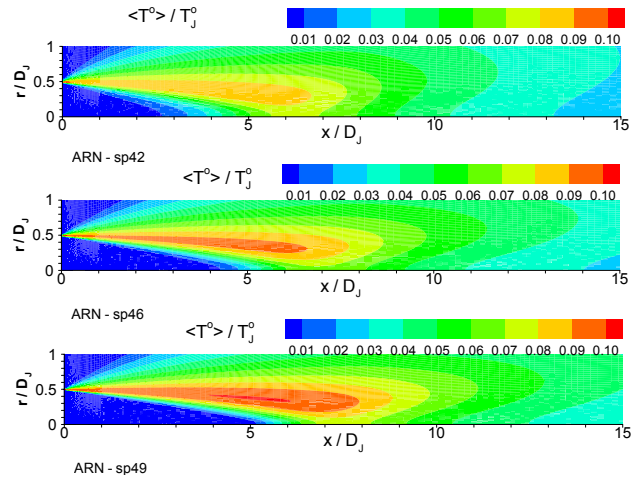
Figure 3. Variance in total temperature normalized with exit total temperature at static temperature ratio of 2.70 and jet acoustic Mach number of: 0.50 (top); 0.90 (middle); and 1.48 (bottom).

IV. Acoustic Results

In the first step, the relative strength of various source terms in the governing wave equation (Eq. 24) will be compared at jet exit conditions shown in Table I. This exercise helps to identify sources that are relatively more important in the noise generation process. The remaining sources will be considered as small and neglected in the final calibration of the prediction methodology.

A. Source Strength Evaluation

Jet noise spectra from various source components are compared at 90° (see Eq. C5, Appendix C). The source correlation coefficient $I_{\eta\eta\eta\eta}$ is replaced with I_{1111} in an isotropic turbulence as described in Appendix B. Both non-compact (Eq. B9) and compact (Eq. B21) variations of the source are considered to in order to ensure that important noise components are not inadvertently overlooked as a result of the specifics of the modeling.

Each row within the column matrix Eq. C5 represents, in an orderly fashion, a source element in Eq. 25. The first and third source terms within the shear noise group are identically zero at $\theta = 90^o$ (i.e., rows 3 and 5 in Eq. C5); and the remaining five sources are integrated over the jet volume starting from its exit plane. The turbulence length- and time-scales are calculated as $\ell = C_\ell \kappa^{1.5} / \varepsilon$ and $\tau_o = C_\tau \kappa / \varepsilon$ for all source elements. Figure 4 shows the relative significance of each source component when a non-compact source model is used. Comparisons point toward *self2* and *shear2* as sources that are relatively small under all conditions, whereas *enthalpy1* and *enthalpy2* intensify with heat and become serious contenders to the *self1* under heated conditions. Between the two heat-related sources, the former scales with ω^4 at low frequency and dominates most of the spectrum – while the latter scales as ω^2 and should be viewed a potential source only at the very early stage of the spectrum. Component predictions shown in Figure 5 use a compact source model (Eq. B21). A similar relative strength among sources is observed, although the spectra appear slightly less broad relative to their respective counterpart in Figure 4.

B. Spectral Predictions

Numerical results are shown for eight subsonic set points described in Table I, and are compared with the lossless, narrow-band measurements of Ref. [4] at a distance of $R/D_j = 100$. In addition to the standard flow variables, which include the turbulent kinetic energy and time- and length-scales, this modified version of the flow solver permitted input of the local total temperature variance as predicted by the modified scalar variance model (Appendix A). Computations use only two source components denoted as *self1* and *enthalpy1*, as represented by the first and the sixth rows in Eq. C5 (Appendix C)

$$\overline{p^2}(\vec{x},\vec{y},\omega) = \frac{\rho_\infty^2 I_{1111} k^4 (1-M^s\cos\theta)^2 (\cos^2\theta + Q\sin\theta)^2}{(4\pi R)^2 (1-M_c\cos\theta)^2} \left[\begin{array}{c} A(\cos^2\theta + Q\sin\theta)^2 \\ +B(1-M^s\cos\theta)^2 \frac{15}{16}\frac{c_\infty^2}{\kappa}\frac{\overline{h_o'^2}}{\tilde{h}^2} \end{array} \right] \sum_{m=0}^{\infty}(1+\delta_{m0})f^m f^{m*}$$

(27)

Outside the usual calibration constants C_ℓ and C_τ that determine the length- and time-scales, the final calibration is achieved by selecting a pair of constants *A* and *B* in Eq. (27), which practically amounts to using a linear combination of the two sources. This is necessary due to the difference in scales between velocity and thermal fluctuations as well as possible cross-correlation between various sources. Parameters *A* and *B* were determined by calibrating the 90° predictions across two set points SP07 and SP27 (Table I).

Spectral results are shown in Figures 6, 7 and 8 for the unheated jets as well as jets at temperature ratio of 1.76 and 2.70. Predictions exhibit a reasonably good agreement with data at angles not very close to the downstream jet axis. The near-axis results weaken gradually with increasing jet speed and/or its temperature. The deteriorating quality of shallow-angles predictions is more likely attributed to the neglect of jet spread in the Green's function calculations which also leads to a dismissal of the causal Green's function. Fine-tunings such as cross-correlation between

sources, or more elaborate statistical models with multiple length-scales and/or non-separable correlations are unlikely to correct the near-axis deficits observed in a parallel flow approximation. The causal solution to the homogeneous parallel-flow equation (20) is known to become unbounded downstream, and is usually discarded as a viable Green's function. A second bounded Green's function is found only when the mean flow supports a small jet spread [Ref. 22]. In that case, a complete solution to the sound field is written as a convolution of the source elements discussed here with both components of the Green's function.

V.   Summary

Identification of the true aerodynamic noise sources is an important aspect of the aeroacoustics research in order to help engine designers with their noise mitigation efforts. Prediction of jet noise from empirical models is a quick and practical way of noise assessment, but is also limited to the bounds of the data-base. The acoustic analogy derivation discussed in section II provides a coherent noise prediction framework that recognizes the sources as the difference between the fluctuating and Favre-averaged Reynolds stresses and enthalpy fluxes. As shown through the component comparisons of section-IV, source elements identified as *self1* and *enthalpy1* in Eq. (25) emerge as the major contributing components to the sound field. This study also highlights the benefits of providing the total temperature fluctuations as a formal input parameter for jet noise prediction from a RANS flowfield simulation. The current approach in extending a baseline scalar variance model to furnish this additional input in a generalized manner is exploratory but appears promising. Needless to say, additional experimental measurements are required to verify the RANS model's quantitative prediction for the temperature fluctuations across a range of propulsive hot jet conditions. Statistical models proposed in the source modeling, although intended to capture the main features of various sources for their strength and spectral roll-off, also require validation. It is hoped that further refinement of the modeling, in conjunction with the instability-related noise component, i.e., convolution of the causal Green's function with the sources described here, could improve spectral predictions at angles close to the jet axis.
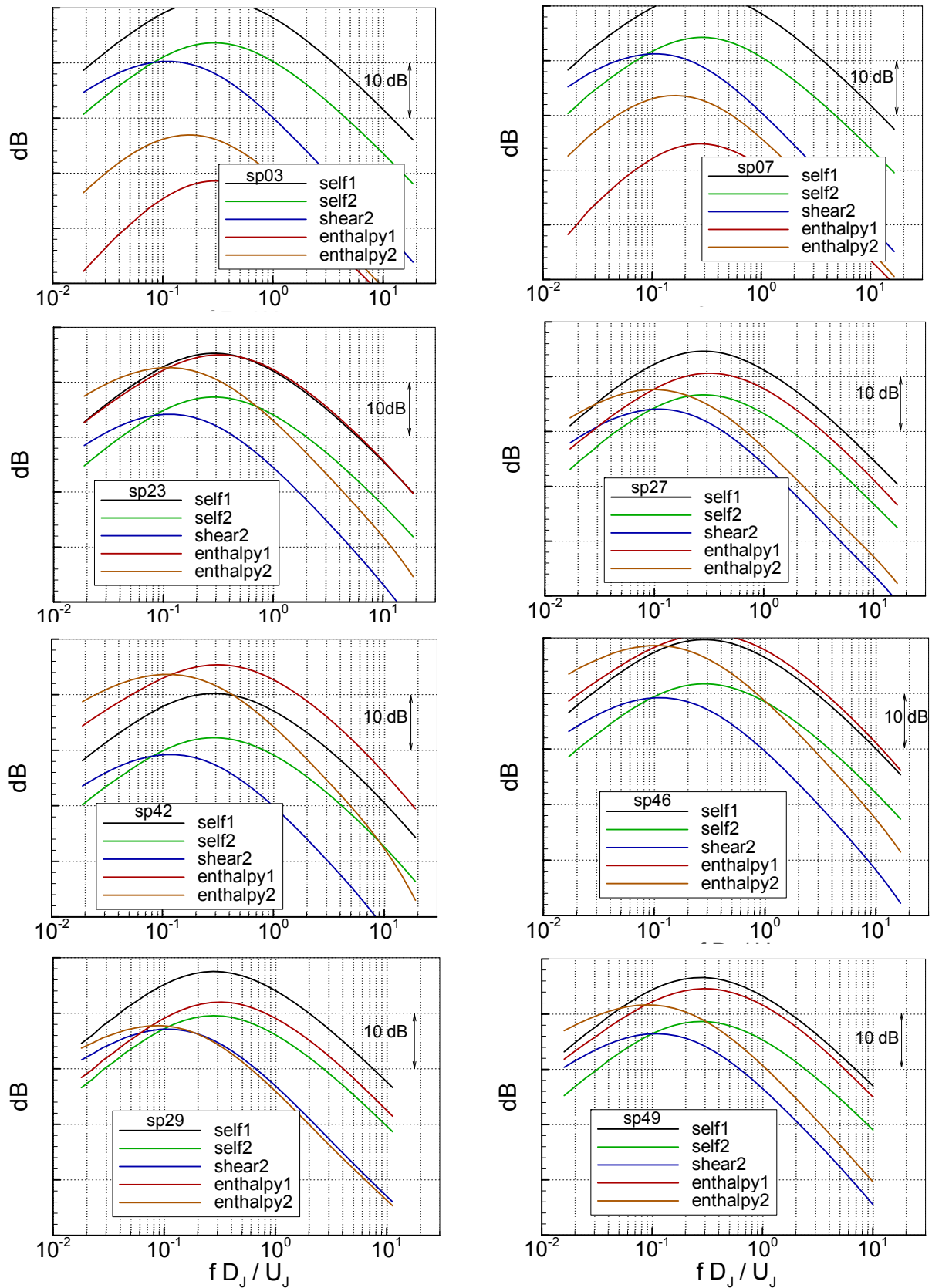
Figure 4. Effect of jet temperature on noise sources in Eq. 26.
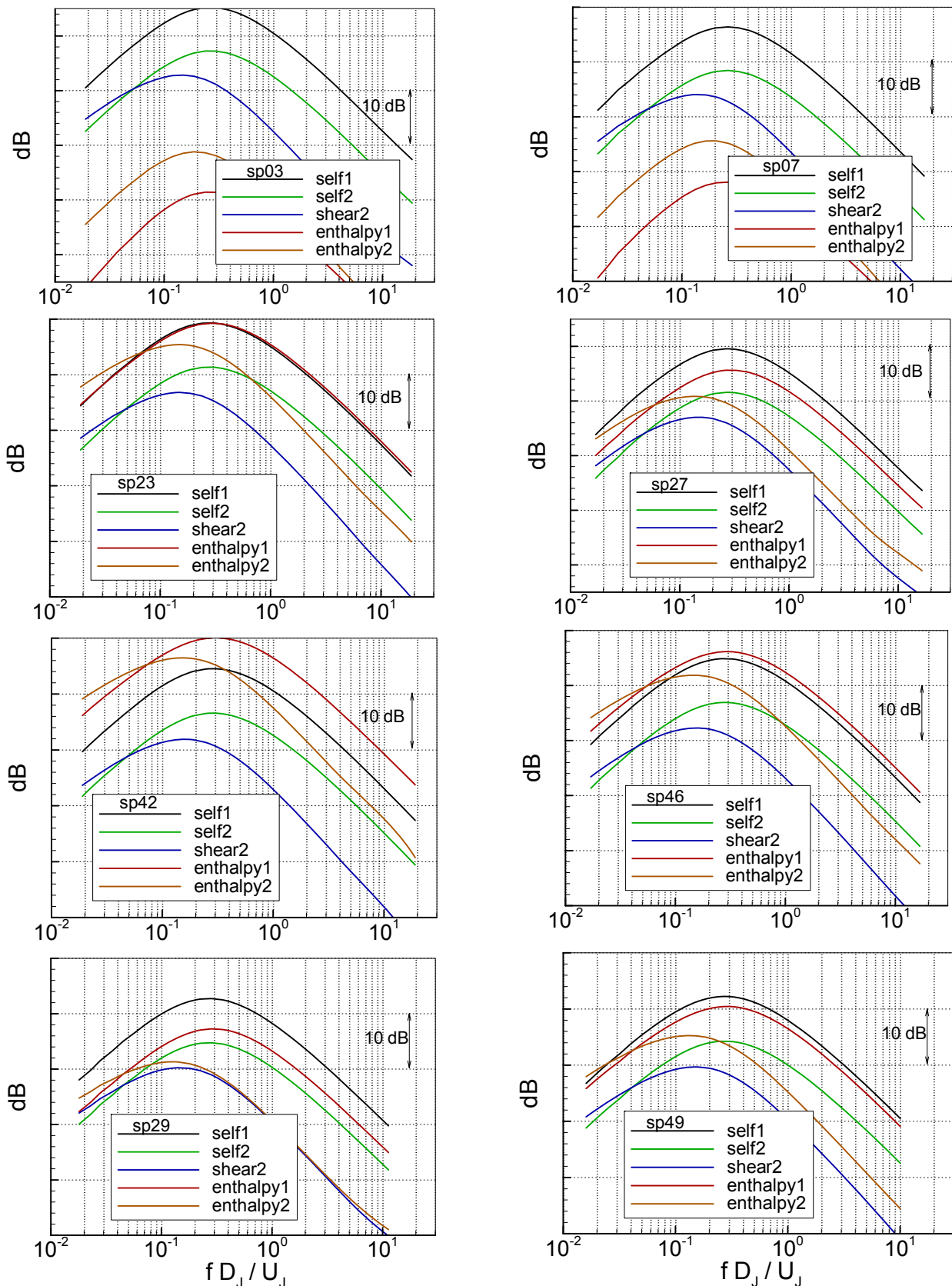Predictions are at 90° observer angle and use a non-compact source model (Eq. B9).

Figure 5. Effect of jet temperature on noise sources in Eq. 26.
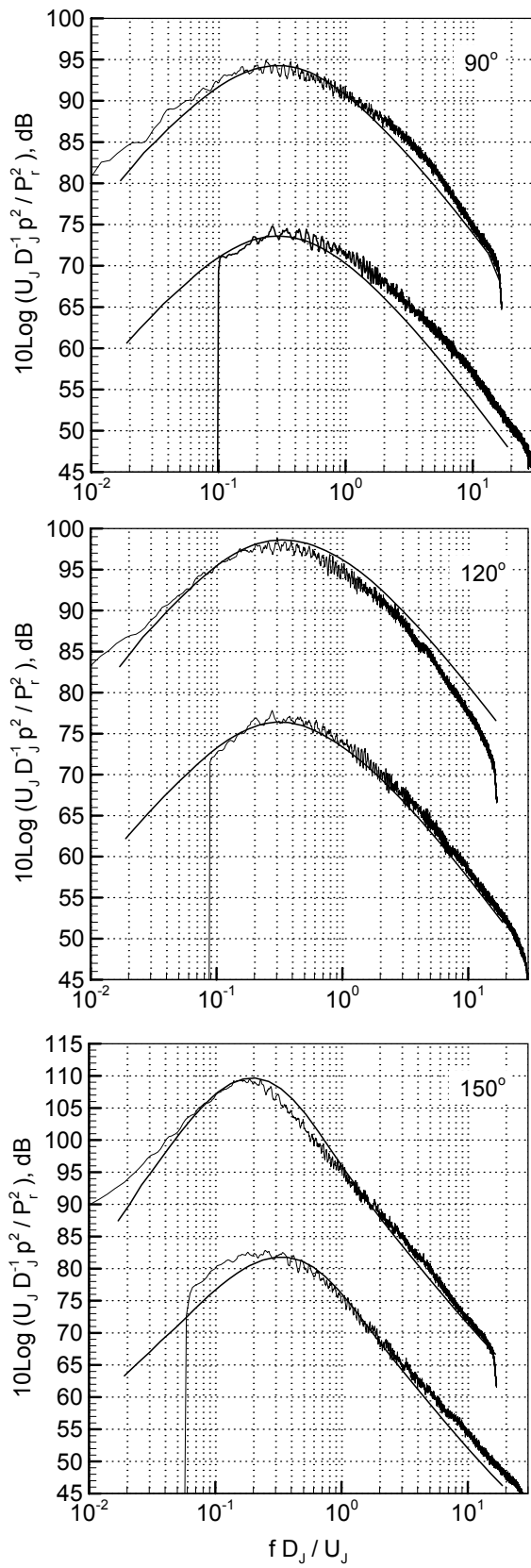Predictions are at 90° observer angle and use a compact source model (Eq. B21).

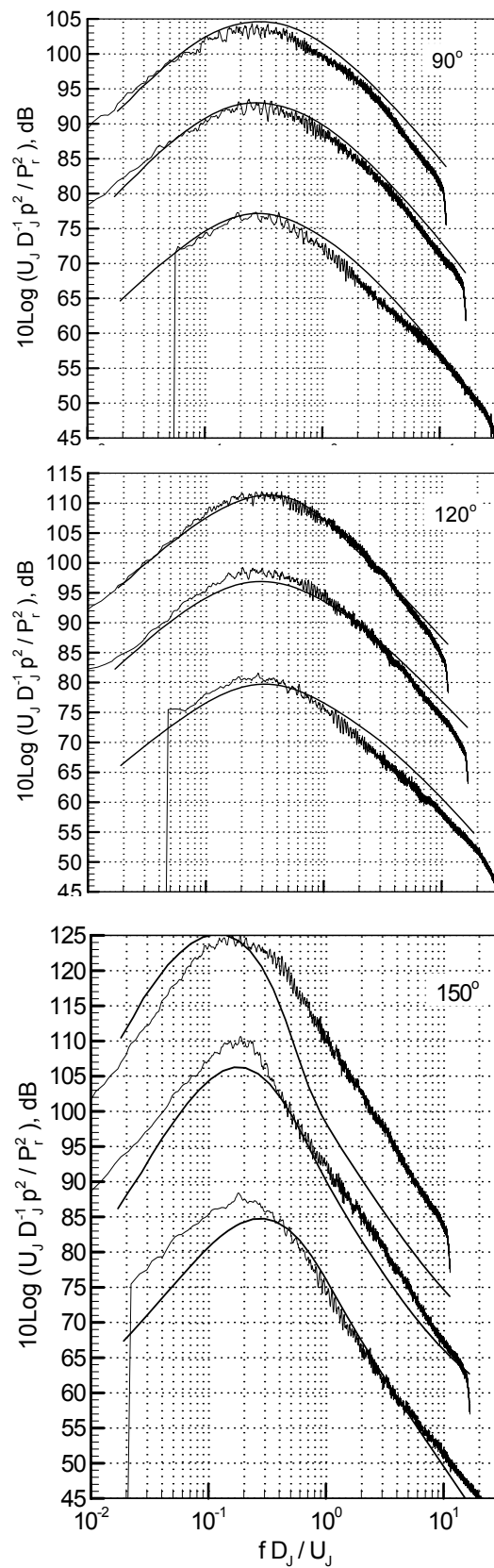**Figure 6. Predicted spectra vs. data at set points SP03 and SP07 at indicated inlet angles.**

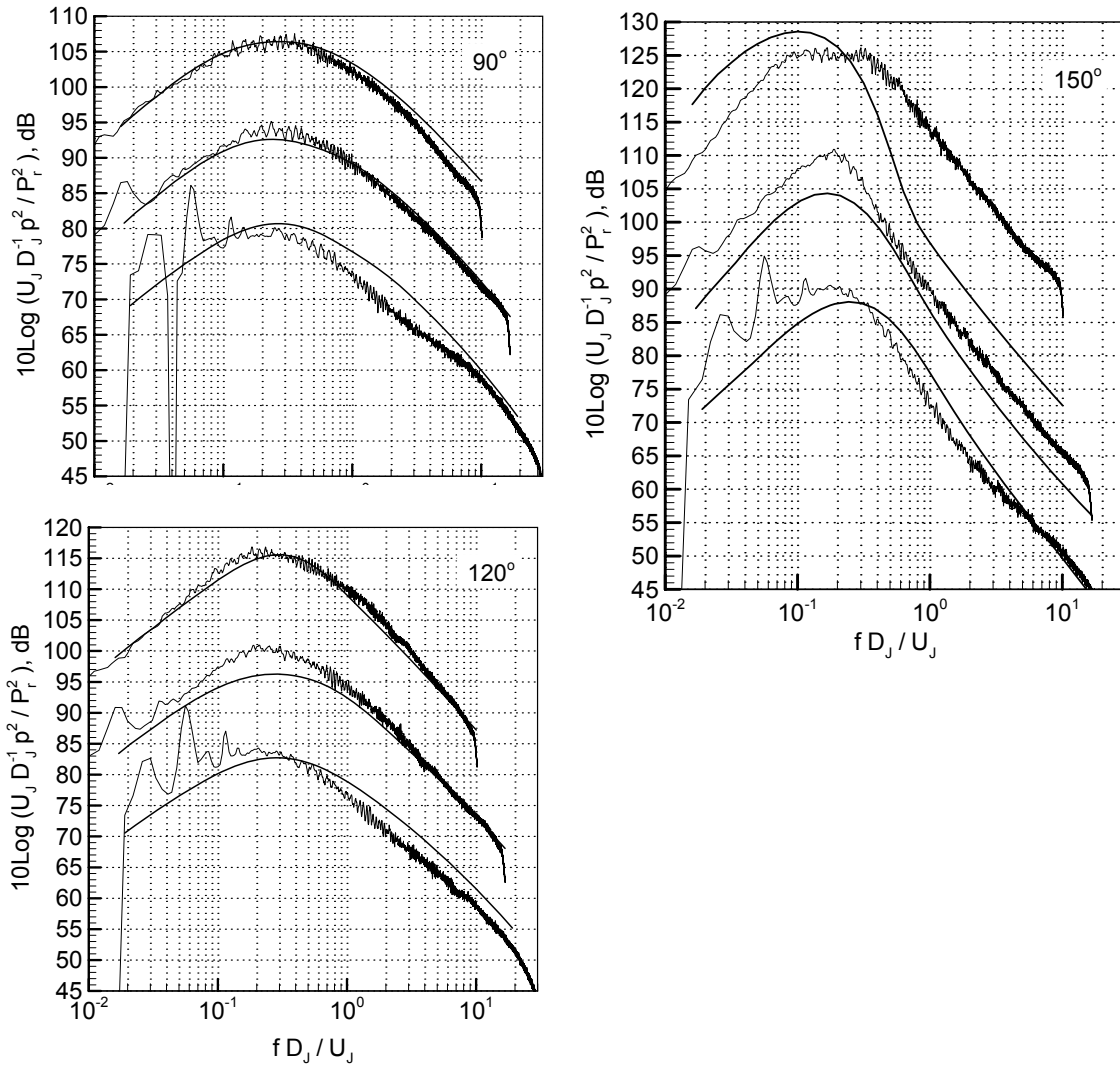**Figure 7. Predicted spectra vs. data at set points SP23, SP27 and SP29 at indicated inlet angles.**

Figure 8.   Predicted spectra vs. data at set points SP42, SP46 and SP49 at indicated inlet angles.

Appendix A – Enthalpy Variance and Dissipation Rate Model

The high-Reynolds-number form of the equations governing the transport of the total enthalpy variance and its dissipation rate is based in concept on the work of Nagano and Kim [13] for generalized turbulent thermal diffusivity

$$\frac{D}{Dt}\rho k_t = \frac{\partial}{\partial x_j}\left[\left(\alpha + \frac{\alpha_t}{\sigma_{kt}}\right)\frac{\partial k_t}{\partial x_j}\right] + P_{k_t} - 2\rho\varepsilon_t \,, \tag{A1}$$

$$\frac{D}{Dt}\rho\varepsilon_t = \frac{\partial}{\partial x_j}\left[\left(\alpha + \frac{\alpha_t}{\sigma_{\varepsilon t}}\right)\frac{\partial\varepsilon_t}{\partial x_j}\right] + \left[\left(\frac{\varepsilon_t}{k_t}\right)\left(C_{d1}\frac{P_{k_t}}{\rho\varepsilon_t} - C_{d2}\right) + \left(\frac{\varepsilon}{k}\right)\left(C_{d3}\frac{P_k}{\rho\varepsilon} - C_{d4}\right)\right]\rho\varepsilon_t \,. \tag{A2}$$

Here, k and ε denote the turbulent kinetic energy (TKE) and dissipation rate obtained from a companion two-equation turbulence model, the operator D/Dt is defined in a similar fashion as D_o in Eq. (7a), α and α_t are the molecular and eddy diffusivities for heat, and P_k is the production term used in the TKE equation. Values utilized for the modeling constants in the variance dissipation rate equation are based on results described in [Refs.1,12] and are listed in Table .

Table A1. Enthalpy Variance Dissipation Rate Coefficient Constants

C_{d1}	C_{d2}	C_{d3}	C_{d4}	σ_{kt}	$\sigma_{\varepsilon t}$
2.0	0.72	2.2	0.8	1.5	1.5

Physical interpretation of the quantity k_t tracked within the CFD simulation is based on selection of the flow variable gradient used for the turbulent variance production term P_{k_t} For example, Nagano and Kim originally solved directly for the static temperature variance. Recent numerical studies modeling helium jets and afterburning rockets plumes indicate improved model generalization using an internal energy variance approach. Further extension of the framework to model the total enthalpy variance was found necessary to improve jet noise prediction.

Two modeling approaches were studied for use in hot jet noise prediction [Ref.1]. The first utilized the internal energy variance as described in [Ref.12]. The second modeled the total enthalpy variance, with appropriate variable substitution for the variance dissipation rate equation. The production term utilized in the total enthalpy variance model is

$$P_{k_t} = 2\alpha_t\frac{\partial h_t}{\partial x_j}\frac{\partial h_t}{\partial x_j} \,, \tag{A3}$$

where e is the specific internal energy and h_t is the specific total enthalpy. For a calorically and thermally perfect gas, the specific heat constants are invariant with temperature, and so the temperature variance can be expressed as f

$$k_t = \overline{h_t' h_t'} = c_p^{\,2}\left(\overline{T_t' T_t'}\right) \,, \tag{A4}$$

and c_p is the specific gas constant. When extending the variance model to predict thermal eddy diffusivity, an expression for the thermal turbulent time scale is needed. Based on results from past work, the following expression was used:

$$\tau_t^2 = \left(\frac{k}{\varepsilon}\right)\max\left[\left(\frac{k_t}{\varepsilon_t}\right),\left(\frac{C_\mu}{C_\lambda}\right)\left(\frac{k}{\varepsilon}\right)\right], \quad C_\mu = 0.09 \tag{A5}$$

The thermal eddy diffusivity, applied to the turbulent diffusion term in the mean energy equation and the variance production term, is written for model closure as

$$\alpha_t = C_\lambda \rho k \tau_t .$$ (A6)

As recommended by Chidambaram *et al.* [23], value of $C_\lambda = 0.14$ was used. The local turbulent Prandtl number is then defined as the ratio of the eddy viscosity to the thermal eddy diffusivity

$$\mathrm{Pr}_t = \mu_t / \alpha_t .$$ (A7)

Appendix B – Source Model

The far-field sound spiral density per unit volume of turbulence at $\vec{y}$ is

$$\overline{p^2}(\vec{x}, \vec{y}, \omega) = \left| G(\vec{x}, \vec{y}, \omega) \right|^2 \int_{\vec{\xi}} \int_{-\infty}^{+\infty} q(\vec{y}, \vec{\xi}, \tau) e^{i\omega\tau} e^{-i\vec{k}\cdot\vec{\xi}} d\tau d\vec{\xi}$$ (B1)

where q denotes a two-point space-time correlation between fluctuating variables at source points A and B separated by space $\vec{\xi}$ and time τ, and G is the relevant Green's function [Ref. 24]. For simplicity, we consider the turbulence as isotropic as described by Batchelor [Ref. 25], and describe a two-point space-time correlation of the velocity components (notation u_i is now used in place of v_i' as a fluctuating velocity component.)

$$\overline{(u_i)_A (u_j)_B} = \overline{u^2}[(f + \tfrac{1}{2}\xi f')\delta_{ij} - \tfrac{1}{2}\frac{\xi_i \xi_j}{\xi} f'],$$

(B2)

$$f'(\xi, \tau) \equiv \frac{\partial f}{\partial \xi}, \quad \xi^2 = \xi_1^2 + \xi_2^2 + \xi_3^2 .$$

Consider a fourth-order time-delayed space-time correlation per unit volume of turbulence at $\vec{y}$

$$R_{ijk\ell}(\vec{y}, \vec{\xi}, \tau) \equiv \overline{u_i u_j u_k' u_\ell'} .$$ (B3)

The spectral density associated with the axial component of the above tensor is the four-dimensional wave-number frequency spectrum function

$$I_{1111}(\vec{y}, \omega^s) = \int_{\vec{\xi}} \int_{\tau} R_{1111}(\vec{y}, \vec{\xi}, \tau) \, e^{i\omega^s \tau} e^{-i\vec{k}\cdot\vec{\xi}} d\tau d\vec{\xi} .$$ (B4)

The above integral was written in a frame moving with source convection velocity U_c, and ω^s is the source frequency in that frame and is related to the observer frequency through the Doppler factor. If turbulence correlation coefficients are *quasi normal,* then the axial component of the above tensor becomes $\overline{u_1 u_1 u_1' u_1'} = 2(\overline{u_1 u_1'})^2$ and subsequently

$$I_{1111}(\vec{y}, \omega^s) = 2(\overline{u_1^2})^2 \int_{\vec{\xi}} \int_{\tau} [(f + \tfrac{1}{2}\xi f') - \tfrac{1}{2}\frac{\xi_1 \xi_1}{\xi} f']^2 e^{i\omega^s \tau} e^{-i\vec{k}\cdot\vec{\xi}} d\tau d\vec{\xi} .$$ (B5)

Similarly, consider the two point space time correlation for the enthalpy/velocity source term

$$\mathfrak{I}_{ij}(\vec{y}, \vec{\xi}, \tau) \equiv \overline{(u_i \frac{h_o'}{\tilde{h}})_A (u_j \frac{h_o'}{\tilde{h}})_B} \cong \frac{1}{\tilde{h}^2} \overline{(u_i h_o')_A (u_j h_o')_B} ,$$ (B6)

$$\Xi_{ij}(\vec{y},\omega^s) \equiv \int\limits_{\vec{\xi}} \int\limits_{\tau} \Im_{ij}(\vec{y},\vec{\xi},\tau) e^{i\omega^s\tau} e^{-i\vec{k}.\vec{\xi}} d\tau d\vec{\xi} . \tag{B7}$$

As suggested by measurements [Ref. 26], we assume that exponential functions govern spatial as well as temporal decay of velocity correlations

$$f(\xi,\tau) = \exp(-\frac{\pi\xi}{\ell} - |\tau/\tau_o|), \quad h(\tau) = \exp(-|\tau/\tau_o|) . \tag{B8}$$

Following Proudman [Ref. 27] the correlation components are considered in the direction of the observer, i.e., the axial component of separation vector aligns with the direction of the wave number $\vec{k}$ (i.e., $\vec{k}.\vec{\xi} = k\xi_1$).

$$I_{1111} = \frac{4\ell^3}{5\pi^2} (\overline{u_1^2})^2 H(\omega^s) N_1(k\ell); \quad H(\omega^s) = \int_{-\infty}^{+\infty} \exp(-2|\frac{\tau}{\tau_o}| + i\omega^s\tau) d\tau = \frac{\tau_o}{1+(\omega^s\tau_o/2)^2} , \tag{B9}$$

where the non-compactness factor N_1 will be defined subsequently. Using Millionshtchikov's hypothesis [Ref. 25] and noting that the autocorrelation of $(u_i h_o')$ is zero in *isotropic turbulence*,

$$\overline{(u_i h_o')_A (u_j h_o')_B} = \overline{(u_i)_A (u_j)_B} \ \overline{(h_o')_A (h_o')_B} . \tag{B10}$$

Now if the space/time correlation governing the enthalpy fluctuations is represented as

$$\overline{(h_o')_A (h_o')_B} = \overline{(h_o')^2} g(\xi,\tau) , \tag{B11}$$

then from Eqs. B6, B7, and B10 we find

$$\Xi_{11}(\vec{y},\omega^s) = \frac{\overline{(h_o')^2}}{\tilde{h}^2} \overline{u_1^2} \int\limits_{\vec{\xi}} \int\limits_{\tau} [(f + \frac{1}{2}\xi f') - \frac{1}{2}\frac{\xi_1\xi_1}{\xi} f'] g(\xi,\tau) e^{i\omega^s\tau} e^{-i\vec{k}.\vec{\xi}} d\tau d\vec{\xi} , \tag{B12}$$

Experimental measurements show that both heated and unheated jets exhibit similar high-frequency decay. Ideally it is desirable for the correlation coefficients B4 and B7 to provide similar asymptotic behavior. In the absence of any experimental data, as a first approximation we assume that enthalpy correlation function $g(\xi,\tau)$ decays in a similar fashion as $f(\xi,\tau)$. From Eq. (B12) it is shown that

$$\Xi_{11}(\vec{y},\omega^s) = \frac{\ell^3}{2\pi^2} (\overline{u_1^2}) \frac{\overline{(h_o')^2}}{\tilde{h}^2} H(\omega^s) N_2(k\ell), \quad g(\xi,\tau) = f(\xi,\tau) . \tag{B13}$$

The non-compactness factors

$$N_1(2\pi\chi) = \frac{5}{8\chi^5} \left[3\tan^{-1}(\chi) - \chi \frac{5\chi^2+3}{(1+\chi^2)^2} \right], \quad N_2(2\pi\chi) = \frac{1}{(1+\chi^2)^2} , \tag{B14}$$

decay as χ^{-5} and χ^{-4} respectively as $\chi \to \infty$.

The spectral shape function due to either self or enthalpy source components is obtained from

$$F(\omega) = \omega^4 H(\omega) N(\frac{\omega}{c_\infty}\ell),$$

(B15)

which shows a low-frequency roll-off $F(\omega) \propto \omega^4$ as $\omega \to 0$. The high-frequency decay is either $F(\omega) \propto \omega^{-3}$ or ω^{-2} depending upon factor N_1 or N_2 (see Eq. B14). The spectral density from above two sources relate as

$$\Xi_{11} = \frac{5}{8}\frac{N_2(k\ell)}{N_1(k\ell)}\frac{1}{\overline{u_1^2}}\frac{\overline{h_o'^2}}{\tilde{h}^2}I_{1111}$$

(B16)

The ratio $N_2(k\ell)/N_1(k\ell)$ remains as 1.0 for most of the spectral range and somewhat beyond the peak, with the exception of the tail-end of the spectrum (Figure B1). In evaluating the relative source strength, this difference has been neglected and the correct high-frequency behavior has been selected as

$$\Xi_{11} \cong \frac{5}{8}\frac{1}{\overline{u_1^2}}\frac{\overline{h_o'^2}}{\tilde{h}^2}I_{1111}.$$

(B17)
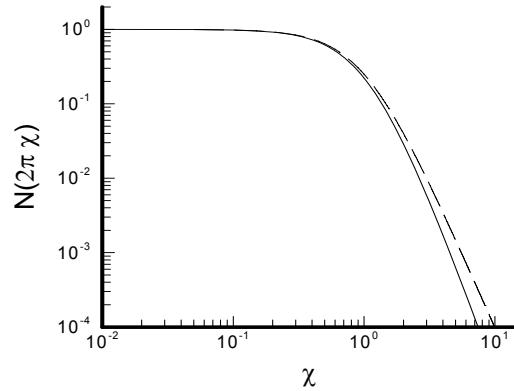
Figure B1.   Non-compactness factor for self and enthalpy source terms (Eq. B14);
solid line, N_1; dashed-line N_2.

In the following discussion, it is shown that alternative function forms are available that are compatible with the exponential functions, and provide similar high-frequency decay for both sources discussed above.

Alternative Source Modeling
A less complicated way of describing the statistical properties of turbulence assumes a compact eddy approximation in the limit of zero wave-number (i.e., $k \to 0$), in which case the non-compactness factors defined in Eq. B14 become identically equal to 1.0. If the correlations were expressed as separable, the spectral density would strongly depend on the temporal function of the correlation for its high-frequency roll-off, and very weakly on its spatial form, as the spatial Fourier transform converts into volume integration. Subsequently, similar spectral characteristics would be expected for both sources.

For example, one may consider a temporal function such as (see Figure B2)

$$h(t,\nu,a) \equiv \frac{(at)^\nu K_\nu(at)}{2^{\nu-1}\Gamma(\nu)}, \quad h(t,\tfrac{1}{2},a) = e^{-at}$$

(B18)

where time t is replaced with its absolute value when it is negative, and K_ν denotes a modified Bessel function. This function is void of a cusp at its origin and its Fourier transform scales as $\omega^{-2\nu-1}$ at high frequency

$$H(\omega) = 2\int_0^\infty h(t,\nu,a)\cos(\omega t)dt = 2\frac{\sqrt{\pi}}{a}\frac{\Gamma(\nu+\frac{1}{2})}{\Gamma(\nu)}\frac{1}{(1+\omega^2/a^2)^{\nu+\frac{1}{2}}} \quad . \tag{B19}$$

The spectral shape function $F(\omega) = \omega^4 H(\omega)$ which would be similar for both correlations B5 and B12, is now modeled by selecting parameter ν. With $\nu = 3$ it is shown that

$$\begin{aligned} F(\omega) &\to \omega^4, \quad \text{as } \omega \to 0 \\ F(\omega) &\to \omega^{-3}, \quad \text{as } \omega \to \infty \end{aligned} \tag{B20}$$
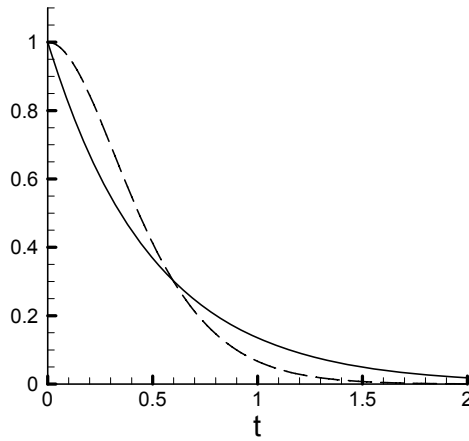
Figure B2. Function $h(t,\nu,a)$ as defined in Eq. (B18); dashed line ($\nu = 3, a = 6$); solid line $\exp(-2t)$.

When $\nu = 11/4$, the high-frequency roll-off follows $F(\omega) \to \omega^{-5/2}$, and source correlation coefficients of interest become

$$\begin{aligned} I_{1111} &= \frac{4\ell^3}{5\pi^2}(\overline{u_1^2})^2 H(\omega^s), \\ \Xi_{11} &= \frac{5}{8}\frac{1}{\overline{u_1^2}}\frac{\overline{h_o'^2}}{\overline{\tilde{h}^2}}I_{1111}, \\ H(\omega^s) &= \frac{\sqrt{\pi}}{3}\frac{\Gamma(13/4)}{\Gamma(11/4)}\frac{\tau_o}{\left(1+(\omega^s\tau_o/6)^2\right)^{13/4}}. \end{aligned} \tag{B21}$$

Appendix C – Source Green's Function Convolution

A stationary point source with frequency ω and location $\vec{x}^s$ (superscript s denotes a source location) is considered in defining the Green's Function (GF)

$$L(\mathbb{G}e^{-i\omega t}) = c_\infty^2 e^{-i\omega t}\delta(\vec{x} - \vec{x}^s),$$

and

$$\mathbb{G}(\vec{x}, \vec{x}^s, \omega) = \frac{1}{4\pi\omega R}e^{ik(R - x_1^s \cos\theta)}\sum_{m=0}^{\infty} f^m(r^s, k, \theta)\cos m(\varphi - \varphi^s),\tag{C1}$$

where $f^m(r^s, k, \theta)$ is solved numerically as a solution to second-order compressible Rayleigh operator [Ref. 24], corresponding to mode number m, wave number $k = \omega/c_\infty$ (to avoid confusion, notation κ will be used to denotes TKE in this appendix), and observer angle θ

$$\frac{d}{dr}\left[\frac{r}{\Phi^2}\frac{dg^m}{dr}\right] + \frac{r}{\Phi^2}\left[k^2(\Phi^2 - \cos^2\theta) - \frac{m^2}{r^2}\right]g^m = 0,$$

$$\Phi^2 \equiv \frac{\rho^s}{\rho_\infty}(1 - M^s \cos\theta)^2, \quad g^m \equiv (1 - M^s \cos\theta)^3 f^m.$$

The relevant GF associated with a moving singularity with source frequency ω^s and convection velocity $\hat{i}U_c$ is

$$L(Ge^{-i\omega t}) = \frac{D}{Dt}\left[c_\infty^2 e^{-i\omega^s t}\delta(x_1 - U_c t)\delta(\vec{x}_t - \vec{x}_t^s)\right],$$

$$G(\vec{x}, \vec{x}^s, \omega) = \frac{-i}{4\pi R}\frac{(1 - M^s \cos\theta)}{(1 - M_c \cos\theta)}e^{ikR}\sum_m f^m(r^s, k, \theta)\cos m(\varphi - \varphi^s),\tag{C2}$$

where $M^s = U(r^s)/c_\infty$ and $M_c = U_c/c_\infty$ are the local acoustic Mach number and convection Mach number respectively. We make the simplifying assumption that the source components on interest are uncorrelated. As usual, the spatial derivatives are moved from source to the Green's function. For example

$$\mathbb{G}\frac{\partial^2 u_i u_j}{\partial x_i \partial x_j} \rightarrow u_i u_j \frac{\partial^2 \mathbb{G}}{\partial x_i \partial x_j}.$$

Some level of simplification is achieved when we consider components of turbulence fluctuations in the direction of the observer θ as suggested by Proudman [Ref. 27]. As an example the first source elements within the self and enthalpy category (see Eq. 27) are designated as $D\dfrac{\partial^2 u_\eta u_\eta}{\partial\eta\partial\eta}$ and $D^2\dfrac{\partial}{\partial\eta}(u_\eta \dfrac{h_o'}{h})$ where η is the component of the spatial separation of the correlation in the direction of the observer (see Figure).
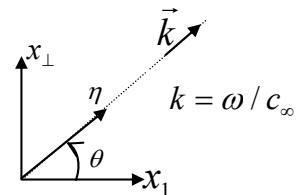
The required spatial derivatives of the Green's function are

$$\mathbb{G}_{,\eta} = \cos\theta \, \mathbb{G}_{,1} + \sin\theta \, \mathbb{G}_{,r}$$

$$\mathbb{G}_{,\eta\eta} = \cos^2\theta \, \mathbb{G}_{,11} + \sin^2\theta \, \mathbb{G}_{,rr} + 2\sin\theta\cos\theta \, \mathbb{G}_{,1r}$$

where $\mathbb{G}_{,1} = -ik\cos\theta \, \mathbb{G}$ and the radial derivative $\mathbb{G}_{,r}$ applies to the function $f^m(r,k,\theta)$.
The following simplifications are introduced into the radial derivatives using the high-frequency solution to the GF

$$f^m_{,r} \cong -ikQf^m, \qquad f^m_{,rr} \cong -(kQ)^2 f^m, \quad Q^2 \equiv \frac{\rho^s}{\rho_\infty}(1-M^s\cos\theta)^2 - \cos^2\theta, \tag{C3}$$

A more accurate representation of function Q should account for mode number

$$Q_m^2 \equiv \frac{\rho^s}{\rho_\infty}(1-M^s\cos\theta)^2 - \cos^2\theta - (\frac{m}{kr})^2. \tag{C4}$$

Since the zeroth mode usually makes the major contribution to the GF, the last term on the RHS was neglected in approximating the derivatives of the GF. Subsequently, the following expression are derived for the far-field spectral density per unit volume ring-source at $\vec{y}$

$$\overline{p^2}(\vec{x},\vec{y},\omega) = \frac{\rho_\infty^2 I_{\eta\eta\eta\eta}}{(4\pi R)^2(1-M_c\cos\theta)^2}
\begin{bmatrix}
k^4(1-M^s\cos\theta)^2(\cos^2\theta+Q\sin\theta)^4 \\[6pt]
+k^4(1-M^s\cos\theta)^6(\frac{c_\infty^2}{\tilde{h}})^2 \\[6pt]
+k^2(\frac{2U_{,r}\sin\theta}{c_\infty})^2\cos^2\theta(\cos^2\theta+Q\sin\theta)^2 \\[6pt]
+k^2(1-M^s\cos\theta)^4(\frac{U_{,r}\sin\theta}{c_\infty})^2(\frac{c_\infty^2}{\tilde{h}})^2 \\[6pt]
+(\frac{2U_{,r}\sin\theta}{c_\infty})^2\cos^2\theta(\frac{\overline{\rho}_{,r}\sin\theta}{\overline{\rho}})^2 \\[6pt]
+k^4(1-M^s\cos\theta)^4(\cos^2\theta+Q\sin\theta)^2\frac{15}{16}\frac{c_\infty^2}{\kappa}\frac{\overline{h_o'^2}}{\tilde{h}^2} \\[6pt]
+k^2(1-M^s\cos\theta)^2(\cos^2\theta+Q\sin\theta)^2(\frac{\overline{\rho}_{,r}\sin\theta}{\overline{\rho}})^2
\end{bmatrix}
\sum_{m=0}^{\infty}(1+\delta_{m0})f^m f^{m*}$$

$$\tag{C5}$$

Each of the seven components shown in the above column matrix represents the contribution to the sound field from a source of Eq. (27) in a similar order. The source correlation coefficient $I_{\eta\eta\eta\eta}$ is the same as I_{1111} in either non-compact (B9) or compact-eddy (B21) representation, and $\kappa = 1.5\overline{u_1^2}$ is the turbulent kinetic energy. The turbulence length- and time-scales are calculated the usual way from the turbulent kinetic energy and its dissipation rate as
$\ell = C_\ell \kappa^{1.5}/\varepsilon$ and $\tau_o = C_\tau \kappa/\varepsilon$.

References

[1] Khavaran, A., and Kenzakowski, D. C., "Progress Toward Improving Jet Noise Prediction in Hot Jets," AIAA-2002-12, January 2007.

[2] Lighthill, M. J., "On Sound Generated Aerodynamically: I. General Theory," Proceedings R. Soc. London, **A211**, pp. 564-587, 1952.

[3] Tanna, H.K., "The Influence of Temperature on Shock-Free Supersonic Jet Noise," J. Sound Vib., **39(4),** pp. 429-460, 1975.

[4] Bridges, J. and Wernet, M. P., "Measurements of the Aeroacoustic Sound Source in Hot Jets," AIAA-2003-3130, May 2003.

[5] Viswanathan, K., "Aeroacoustics of Hot Jets," J. Fluid Mechanics, **519**, pp.39-82, 2004.

[6] Viswanathan, K. "Improved Method for Prediction of Noise from Single Jets," AIAA Journal, **45(1)**, pp. 151-161, 2007.

[7] Tam, C. K.W., "Dimensional Analysis of Jet Noise Data,"AIAA-2005-2938, May 2005.

[8] Morfey, C. L., and Szewczyk, V. M., "New Scaling Laws for Hot and Cold Jet Mixing Noise Based on a Geometric Acoustic Model, " J. Sound Vib., **61(2)**, pp. 255-292, 1978.

[9] Lush, P. A., and Fisher, M. J., AGARD CP-131 (Noise Mechanisms), Chapter 12: Noise from Hot Jets, 1973.

[10] Lilley, G. M., "The Radiated Noise from Isotropic Turbulence with Application to the Theory of Jet Noise," J. Sound Vib., **190(3)**, pp. 463-476, 1996.

[11] Goldstein, M. E., "A Generalized Acoustic Analogy," J. Fluid Mechanics, **488**, pp. 315-333, 2003.

[12] Kenzakowski, D.C., "RANS Modeling Improvements for Jets Using Scalar Variance Equations,AIAA-2006-0491, Jan. 2006.

[13] Nagano, Y. and Kim. C., "A Two-Equation Model for Heat Transport in Wall Turbulent Shear Flows," J. Heat Transfer, **(110)**, pp. 583-589, 1988.

[14] Lilley, G. M., "Jet noise: Classical Theory and Experiments," NASA Reference Publication 1258, (*Aeroacoustics of Flight Vehicles, Theory and Practice*), Vol. 1, pp. 211-289, 1991.

[15] Farassat, F., Doty, M. L., and Hunter, C. A. "The Acoustic Analogy – A Powerful Tool in Aeroacoustics with Emphasis on Jet Noise Prediction," AIAA-2004-2872, May 2004.

[16] Freund, J. B., "Noise-Source Turbulence Statistics and the Noise from a Mach 0.90 Jet," Journal of Physics of Fluids, **15(5)**, pp. 1788-1799, 2003.

[17] Lew, P., Blaisdell, G. A., and Lyrintzis, A. S., "Investigation of Noise Sources in Turbulent Hot Jets Using Large Eddy Simulation Data," AIAA-2007-16, January 2007.

[18] Tanna, H. K., "An Experimental Study of Jet Noise, Part I: Turbulent Mixing Noise," J. Sound Vib., **50(3)**, pp. 405-428, 1977.

[19] Kenzakowski, D.C., "Turbulence Modeling Improvements for Jet Noise Prediction Using PIV Datasets," 10th AIAA/CEAS Aeroacoustics Conf., AIAA-2004-2978, May 2004.

[20] Bridges, J., "Effect of Heat on Space-Time Correlation in Jets," AIAA-2006-2534, May 2006.

[21] Witze, P. O., "Centerline Velocity Decay of Compressible Free Jets," AIAA Journal, **12(4)**, pp. 417-418, 1974.

[22] Goldstein, M. E., and Leib, S. J., "The Role of Instability Waves in Predicting Jet Noise," J. Fluid Mechanics, **525**, pp. 37-72, 2005.

[23] Chidambaram N., Dash, S.M., and Kenzakowski, D.C., "Scalar Variance Transport in the Turbulence Modeling of Propulsive Jets," J. Propulsion & Power, Jan - Feb., 2001.

[24] Khavaran, A., Georgiadis, N. J., Bridges, J., and Dippold, V. F., "Effect of Free Jet on Refraction and Noise," AIAA-2005-2941, May 2005.

[25] Batchelor, G. K., *The Theory of Homogeneous Turbulence*, Cambridge University Press, 1953.

[26] Bridges, J., and Wernet, M. P., "Turbulence Measurements of Separate Flow Nozzles with Mixing Enhancement Features," AIAA-2002-2484, June 2002.

[27] Proudman, I., "The Generation of Noise by Isotropic Turbulence," The Proceeding of the Royal Society of London, **A214**, pp. 119-132, 1952.

REPORT DOCUMENTATION PAGE

1. REPORT DATE *(DD-MM-YYYY)* 09-07-2007	2. REPORT TYPE Final Contractor Report	3. DATES COVERED *(From - To)*

4. TITLE AND SUBTITLE Noise Generation in Hot Jets	5a. CONTRACT NUMBER NNC06BA07B
	5b. GRANT NUMBER
	5c. PROGRAM ELEMENT NUMBER
6. AUTHOR(S) Khavaran, Abbas; Kenzakowski, Donald, C.	5d. PROJECT NUMBER
	5e. TASK NUMBER
	5f. WORK UNIT NUMBER WBS 561581.02.08.03.18.03

7. PERFORMING ORGANIZATION NAME(S) AND ADDRESS(ES) ASRC Aerospace Corporation 21000 Brookpark Road Cleveland, Ohio 44135	8. PERFORMING ORGANIZATION REPORT NUMBER E-16145

9. SPONSORING/MONITORING AGENCY NAME(S) AND ADDRESS(ES) National Aeronautics and Space Administration Washington, DC 20546-0001	10. SPONSORING/MONITORS ACRONYM(S) NASA
	11. SPONSORING/MONITORING REPORT NUMBER NASA/CR-2007-214924; AIAA-2007-3640

12. DISTRIBUTION/AVAILABILITY STATEMENT
Unclassified-Unlimited
Subject Categories: 71 and 01
Available electronically at http://gltrs.grc.nasa.gov
This publication is available from the NASA Center for AeroSpace Information, 301-621-0390

13. SUPPLEMENTARY NOTES

14. ABSTRACT
A prediction method based on the generalized acoustic analogy is presented, and used to evaluate aerodynamic noise radiated from high speed hot jets. The set of Euler equations are split into their respective non-radiating and residual components. Under certain conditions, the residual equations are rearranged to form a wave equation. This equation consists of a third-order wave operator, plus a number of non-linear terms that are identified with the equivalent sources of sound and their statistical characteristics are modeled. A specialized RANS solver provides the base flow as well as turbulence quantities and temperature fluctuations that determine the source strength. The main objective here is to evaluate the relative contribution from various source elements to the far-field spectra and to show the significance of temperature fluctuations as a source of aerodynamic noise in hot jets.

15. SUBJECT TERMS
Noise; Jet noise; Propulsion noise; Flow noise

16. SECURITY CLASSIFICATION OF:			17. LIMITATION OF ABSTRACT	18. NUMBER OF PAGES	19a. NAME OF RESPONSIBLE PERSON Abbas Khavaran
a. REPORT U	b. ABSTRACT U	c. THIS PAGE U		31	19b. TELEPHONE NUMBER *(include area code)* 216-977-1120